

## THEORETICAL CHARACTERIZATION OF INFILL PANELS BASING ON COMPRESSIVE AND SHEAR TESTS

T. Albanesi<sup>1</sup>, A.V. Bergami<sup>2</sup>, S. Biondi<sup>3</sup>, E. Candigliota<sup>4</sup>, C. Nuti<sup>5</sup>

<sup>1</sup> Assistant Professor, Department of Structures, Dis, University of Roma Tre, Rome, Italy

<sup>2</sup> Ph. D. in Structural Engineering, Department of Structures, Dis, University of Roma Tre, Rome, Italy

<sup>3</sup> Associate Professor, Department of Design, Rehabilitation and Control of Architectural Structures, Pricos, University "G. D'Annunzio", Chieti-Pescara, Italy

<sup>4</sup> Ph.D. in Structural Engineering, Pricos Department, University "G.D'Annunzio", Chieti-Pescara, Italy

<sup>5</sup> Full Professor, Department of Structures, Dis, University of Roma Tre, Rome, Italy

Email: t.albanesi@uniroma3.it, abergami@uniroma3.it, s.biondi@pricos.unich.it, e.candigliota@unich.it, c.nuti@uniroma3.it

### ABSTRACT:

This paper discusses the orthotropic behavior of a kind of infill panels: in particular slender clay brick panels are analyzed in order to calibrate the mechanical characteristics required in force-displacement relationship for an infilled RC frame. Two different kinds of clay brick panels (120 mm thick with semi-solid bricks and 80 mm thick with hollow bricks) have been tested in the two orthogonal (in plane) principal directions and in the diagonal direction. Components were tested too: bricks in compression and mortar both in compression and bending. The results of this test sequence were discussed in the past in terms of components-to-panel compressive strength ratio. In this paper test results in terms of orthotropic plane behavior are discussed and some criteria to define the elastic characteristic are pointed out.

**KEYWORDS:** structural response, masonry panels, infilled RC frames, compressive test, shear test

### 1. INTRODUCTION

Numerous experimental tests on infill panels were performed at the *Laboratory of Experiments on Materials and Structures* of Roma Tre University, these tests are part of a wider research program called "Ecoleader" that was carried out at the CEA Laboratory of Saclay. Further test sequence on brick components is carrying out at the *Scam Structural Laboratory* of Chieti-Pescara University. Tests aim to study RC frames - infill masonry interaction and to define a correct numerical approach for this kind of structures. The research team focused the attention on brick and mortar mechanical characteristics in order to define infill panel characteristics.

Some correlation formulas have been extensively discussed in the past including infill slenderness effects (Biondi et al. 2002) and were used for RC frame modeling and structural analysis (Albanesi et al. 2006, 2008a). More recently orthotropic bi-dimensional behavior of infill panels was taken into account. Horizontal, vertical and diagonal compressive tests have been performed on infill specimens with at least five mortar layers. Tests results in terms of compressive panel strength based on brick and mortar strengths were discussed in Albanesi et al. 2008b. In this paper the orthotropic behavior of infill panels is pointed out and an original homogenization criterion is discussed in order to define an useful approach in numerical analysis of infilled RC homogenization criterion is discussed in order to define an useful approach in numerical analysis of infilled RC frames.

### 2. ORTHOTROPIC MODEL FOR MASONRY IN-PLANE ELEMENTS

In presence of a seismic action, an infill panel sustains an in-plane loading condition: a vertical component due to gravity loads and a horizontal load due to RC frame - infill panel seismic interaction. Thus an in-plane stress-stress condition can be assumed in analysis and constitutive equations can be written as:

$$\sigma_i = C_{ij} \varepsilon_j \qquad \varepsilon_i = D_{ij} \sigma_j \qquad (2.1)$$

where  $\boldsymbol{\sigma} = \{\sigma_i, \sigma_j, \sigma_{ij}\}^T$  and  $\boldsymbol{\varepsilon} = \{\varepsilon_i, \varepsilon_j, \varepsilon_{ij}\}^T$  are the in-plane stress and strain tensors respectively,  $\mathbf{C}$  = stiffness matrix and  $\mathbf{D}$  = compliance matrix:

$$\mathbf{C} = \begin{bmatrix} \frac{E_{ii}}{1-\nu_{ij}\nu_{ji}} & \frac{\nu_{ij}E_{ii}}{1-\nu_{ij}\nu_{ji}} & 0 \\ \frac{\nu_{ji}E_{jj}}{1-\nu_{ij}\nu_{ji}} & \frac{E_{jj}}{1-\nu_{ij}\nu_{ji}} & 0 \\ 0 & 0 & 2G_{ij} \end{bmatrix} \quad \mathbf{D} = \begin{bmatrix} \frac{1}{E_{ii}} & -\frac{\nu_{ij}}{E_{jj}} & 0 \\ -\frac{\nu_{ji}}{E_{ii}} & \frac{1}{E_{jj}} & 0 \\ 0 & 0 & \frac{1}{2G_{ij}} \end{bmatrix} \quad (2.2)$$

If elastic range is considered in these matrixes five independent terms can be defined:  $E_{ii}$  and  $E_{jj}$  longitudinal elastic moduli,  $\nu_{ij}$  and  $\nu_{ji}$  Poisson's ratios ( $-\nu_{ij}$  represents the ratio between  $i$ -direction to  $j$ -direction deformations),  $G_{ij}$  shear modulus. Due to compliance matrix symmetry it is possible to assume:

$$\frac{\nu_{ij}}{E_{jj}} = \frac{\nu_{ji}}{E_{ii}} \quad \frac{D_{ij}}{D_{ji}} = 1 \quad (2.3)$$

and consequently to obtain symmetrical matrixes defined by means of four independent terms

Notice that a violation of tensorial invariance is generally detected for fragile materials like infill walls (Bažant 1983); this topic will be discussed later, basing on test results. Stress and strain components in a  $Ox_hx_k$  Cartesian system obtained with a rigid rotation  $\theta$  of the  $Ox_ix_j$  Cartesian system can be defined as:

$$\sigma_{hk} = \sigma_{ij}n_{ih}n_{jk} \quad \varepsilon_{hk} = \varepsilon_{ij}n_{ih}n_{jk} \quad (2.4)$$

where the direction cosines, for a positive counterclockwise rotation, can be defined as:

$$n_{ih} = x_{i,h} = n_{jk} = x_{j,k} = \cos\theta \quad n_{ik} = x_{i,k} = n_{jh} = x_{j,h} = -\sin\theta \quad (2.5)$$

In this  $\theta$  rotate direction, the longitudinal elastic modulus,  $E_{hh}$ , can be defined as:

$$E_{hh} = \left[ \frac{\cos^4\theta}{E_{ii}} + \frac{\sin^4\theta}{E_{jj}} + \sin^2\theta \cos^2\theta \left( \frac{1}{G_{ij}} - 2\frac{\nu_{ij}}{E_{jj}} \right) \right]^{-1} \quad (2.6)$$

and can be used for example in an equivalent strut model (single or multiple) approach (Biondi et al. 2006).

As above pointed out, four independent terms have to be defined for an orthotropic medium by means of tests while no relationship can be defined between elastic moduli and shear modulus as for an isotropic medium:

$$G = \frac{E}{2(1+\nu)} \quad (2.7)$$

For this reason shear test should be carried out in order to use (2.1)÷(2.2) in the case of orthotropic material, unfortunately direct shear tests on fragile clay bricks panel specimens are not as simple and stable as compressive tests, so indirect longitudinal shear tests have to be carried out.

In order to avoid this shear test necessity, some authors suggested (Pietruszczak et al. 1992, Anthoine 1995) to derive the in-plane elastic characteristics of masonry by means a homogenization theory: this theory for periodic media allows the global behavior of masonry to be derived from the elastic behavior of brick and mortar.

Then, in the case of a solid brick masonry, components can be assumed to be isotropic medium and their elastic characteristics  $E_m$ ,  $\nu_m$ ,  $G_m$  (for mortar) and  $E_b$ ,  $\nu_b$ ,  $G_b$  (for brick) can be used for masonry wall characterization. According to a proposal, useful in the inelastic range too (Gambarotta et al. 1997), the elastic masonry characteristics can be approximated as:

$$E_{wii} = \eta_{mi} E_m + \eta_{bi} E_b \quad E_{wjj} = \left[ \frac{\eta_{bi}}{E_b} + \frac{\eta_{mi}}{E_m} - \frac{\eta_{mi} \eta_{bi} E_m E_b}{E_{wii}} \left( \frac{\nu_b}{E_b} - \frac{\nu_m}{E_m} \right)^2 \right]^{-1} \quad (2.8)$$

$$\nu_{wji} = \eta_m \nu_m + \eta_b \nu_b \quad G_{wjj} = \left( \frac{\nu_m}{G_m} + \frac{\nu_b}{G_b} \right)^{-1} \quad (2.9)$$

where  $\eta_{mi}$  is the mortar-to-brick volume ratio:

$$\eta_{mi} = \frac{s_{mj}}{s_{mj} + s_{bj}} \quad \eta_{bi} = 1 - \eta_{mi} \quad (2.10)$$

being  $s_{mj}$  and  $s_{bj}$  the mortar joint and brick heights in  $j$ -direction (normal to bed joints) respectively. In the case of hollow and semi-solid bricks panels not only the mortar volume ratio is very low but also the brick component is an orthotropic medium. For this reason Biondi et al. (2006) proposed a different criterion for infill panel homogenization. This criterion will be theoretically outlined in the next paragraph and experimentally evaluated in the next Chapter. It has to be noted that this hypothesis showed a good agreement with RC frame experimental data if it has been used in numerical analyses (Albanesi et al. 2006).

### 2.1. Homogenization criterion based on characteristic compressive strength

Disregarding any aspect ratio of brick components in shear test (Figure 2 and Figure 3 show that shear specimen hasn't a polar symmetry with respect to plane normal  $k$ -direction), elastic moduli can be determined in terms of characteristic compressive strength of masonry as suggest by Italian Code (IC) and Eurocode 6 (EC6):

$$E_{wi} = 1000 f_{wki} \quad E_{wj} = 1000 f_{wkj} \quad (2.11)$$

where  $i$  and  $j$  identify (throughout the rest of this paper) the horizontal and vertical directions respectively (which alternatively are the strong and weak directions in these test series, due to vertical testing machine load direction). A simple relationship between shear modulus and elastic modulus is assumed in these Codes too:

$$G = 0.40E \quad (2.12)$$

Using (2.12) for each direction, an average value of the shear modulus and Poisson's ratio can be derived:

$$G_{wjj} = 0.40 \left( \frac{E_{wi} + E_{wj}}{2} \right) = \frac{1}{2} \left[ \frac{E_{wi}}{2(1+\nu_w)} + \frac{E_{wj}}{2(1+\nu_w)} \right] \quad \nu_w = \frac{\nu_{wij} + \nu_{wjj}}{2} = 0.25 \quad (2.13)$$

Finally the two unknown orthotropic Poisson's ratios can be defined:

$$\nu_{wij} = \frac{2\nu_w}{\left( 1 + \frac{E_{wi}}{E_{wj}} \right)} \quad \nu_{wji} = \frac{2\nu_w}{\left( 1 + \frac{E_{wj}}{E_{wi}} \right)} \quad (2.14)$$

in order to calculate the equivalent diagonal elastic modulus  $E_{w\theta} = E_{hh}$  by means of (2.6) and then to derive the diagonal compressive strength which is useful for structural analysis:

$$f_{w\theta} = \frac{E_{w\theta}}{1000} \quad (2.15)$$

### 2.2. Homogenization criterion evaluation based on test results

Test program and tests results on components and masonry were partially shown and discussed in Albanesi et al. (2008.a), together with a description of the testing machine, laboratory apparatus and stress-strain curves. In this paper some remarks will be pointed out to evaluate the proposed homogenization criterion (2.11)÷(2.15).

Two kinds of tests were carried out on mortar: three points bending tests (support span  $100 \pm 5$  mm) on prismatic  $40 \times 40 \times 160$  mm<sup>3</sup> specimens and compression tests on cylindrical  $100 \times 200$  mm<sup>2</sup> specimens: due to test results mortar was then classified as M20 (i.e., very high quality). Test results in terms of flexural tensile strength,  $f_{mf}$ , compressive uniaxial strength,  $f_m$ , flexural and compressive characteristic strengths ( $f_{mfk}$ ,  $f_{mk}$ ) are summarized in Table 1; the characteristic value is obtained from the average one, depending on specimens population or Code provisions, as:

$$f_k = \min \{ \alpha f_m; f_m + k\sigma \} \quad (2.16)$$

Two kinds of common clay bricks have been tested: hollow non-structural bricks ( $80 \times 160 \times 330$  mm<sup>3</sup> horizontally perforated units with rendering keyways, 6 holes,  $\phi = 58\%$  hollow percentage) and semi-solid bricks ( $120 \times 120 \times 250$  mm<sup>3</sup> vertically perforated units with single grip hole,  $\phi = 49\%$  hollow percentage). A half of each brick group was tested in holes direction (strong direction tests) and the other half in perpendicular in-plane direction (weak direction tests). Test results are shown in Table 1 using the same notation as for mortar. In the past (Biondi et al. 2002, Biondi et al. 2006, Albanesi et al. 2008.a) some correlations between compression strength of component elements (brick and mortar) and masonry mechanical characteristics were discussed paying particular attention to infill slenderness effects on masonry strength.

Three relationships were selected for this scope: the Italian Code (IC) functional relationship (2.17), the Eurocode 6 (EC6) explicit relationship (2.18) and the relationship (2.19) (valid for medium strength elements, Tassios 1998). In (2.17) and (2.18) the panel slenderness influence is not explicit while in (2.20) it is considered in terms of panel height-to-thickness ratio ( $h_w/t_w$ ):

$$f_{wk} = f(f_{bk}; f_{mm}) \quad (2.17)$$

$$f_{wk} = k(\delta f_{bm})^\alpha f_{mm}^\beta \quad (2.18)$$

$$f_w = f_b \left( \frac{4 + 0.10 f_m}{12 + 5 h_w/t_w} \right) + 2 \quad (2.19)$$

Table 1. Compression test results on components and masonry panels (in MPa)

| mortar tests |                | brick strong compressive tests |          |                   |          | brick weak compressive tests |          |                   |          |
|--------------|----------------|--------------------------------|----------|-------------------|----------|------------------------------|----------|-------------------|----------|
| flexural     |                | hollow bricks                  |          | semi-solid bricks |          | hollow bricks                |          | semi-solid bricks |          |
| $f_{mf}$     | $f_{mfk}$      | $f_{bm}$                       | $f_{bk}$ | $f_{bm}$          | $f_{bk}$ | $f_{bm}$                     | $f_{bk}$ | $f_{bm}$          | $f_{bk}$ |
| 4.82         | 3.37           | 10.40                          | 6.07     | 23.39             | 20.17    | 4.97                         | 2.55     | 5.11              | 2.56     |
| compressive  |                | panel strong compressive tests |          |                   |          | panel weak compressive tests |          |                   |          |
| $f_m$        | $f_{mk}$       | hollow panels                  |          | semi-solid panels |          | hollow panels                |          | semi-solid panels |          |
| 23.49        | 15.89          | $f_{wm}$                       | $f_{wk}$ | $f_{wm}$          | $f_{wk}$ | $f_{wm}$                     | $f_{wk}$ | $f_{wm}$          | $f_{wk}$ |
|              | <i>Exp.</i>    | 3.11                           | 2.59     | 7.95              | 6.63     | 2.24                         | 1.78     | 3.08              | 2.56     |
|              | <i>IC</i>      | 3.61                           | 3.01     | 15.71             | 13.09    | 1.47                         | 1.16     | 1.98              | 1.65     |
|              | <i>EC6</i>     | 6.86                           | 5.72     | 12.03             | 10.02    | 3.42                         | 2.85     | 3.99              | 3.32     |
|              | <i>Tassios</i> | 2.88                           | 2.30     | 5.37              | 4.30     | 2.42                         | 1.94     | 2.74              | 2.19     |

In Table 1, (2.17)-(2.19) theoretical results are compared with experimental ones. Mpa are used. The IC provision is in good agreement with experimental results for hollow panels while the EC6 is more efficient, even with some over-estimation, for semi-solid panels.

$$f_{wk} = \min \left\{ \frac{f_{wm}}{1.20}; \frac{\min \{ f_{wi} \}}{0.90} \right\} \quad (2.20)$$

Due to the small number of specimens, the (2.20) conventional relationship is used, according to Italian Code in order to obtain both experimental values and characteristic theoretical values.

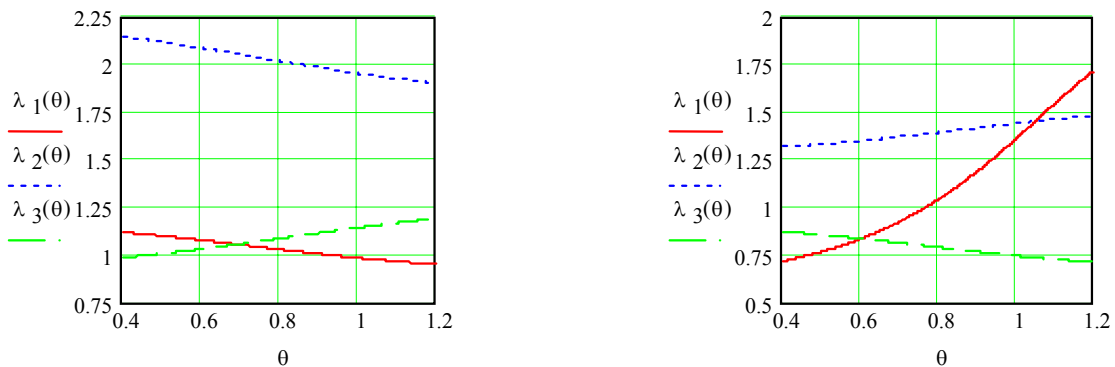


Figure 1. Equivalent diagonal elastic modulus ratios for hollow (left) and semi-solid (right) panels

A comparison of diagonal elastic modulus ratios ( $\lambda_1 = E_{w\theta IC} / E_{w\theta exp}$  solid line,  $\lambda_2 = E_{w\theta EC6} / E_{w\theta exp}$  dot line,  $\lambda_3 = E_{w\theta T} / E_{w\theta exp}$  dashed line) is shown in Figure 1. Diagonal elastic modulus is obtained using (2.6) and homogenization criteria (2.11)÷(2.15) for experimental data ( $E_{w\theta exp}$ ), Italian Code ( $E_{w\theta IC}$ ), Eurocode 6 ( $E_{w\theta EC6}$ ) and Tassios ( $E_{w\theta T}$ ) in the range  $\theta = \tan^{-1}\{h_w / l_w = 0.50; h_w / l_w = 2.00\}$ .

The efficiency of Italian Code provisions is similar to Tassios provision due to the balance of IC overestimation in strong direction and underestimation in weak direction. EC6 provision has a lower efficiency due to a general overestimation of masonry panel strength.

### 3. ORTHOTROPIC MODEL DISCUSSION BASED ON IN-PLANE TESTS

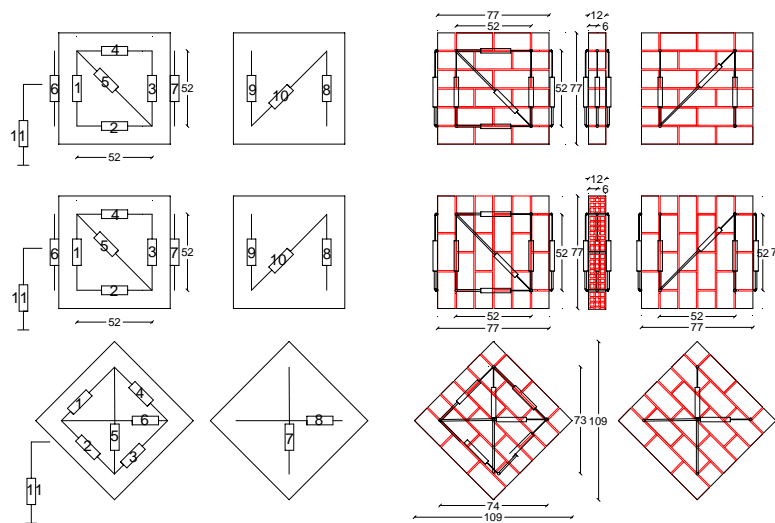


Figure 2. Specimen geometry and displacement transducers disposal for semi-solid panels: strong direction (top), weak direction (middle) and diagonal direction (bottom) [vertical loading direction]

Globally 24 infill square panels with 5÷10 mm thick mortar layers have been built using the previously described bricks and mortar: 12 hollow panels  $1010 \times 1010 \times 800 \text{ mm}^3$  (horizontal holes), 12 semi-solid panels  $770 \times 770 \times 120 \text{ mm}^3$  (vertical holes). Panels were tested in compression, in both strong and weak directions, and in the diagonal one by means of a load-control testing machine. A redundant number of displacement transducers (linear potentiometer with  $\pm 50 \text{ mm}$  stroke) have been placed with hinged-ends and measure bases are so long as to include at least 3 mortar layers in hollow direction. As shown in Figure 2 and Figure 3, 10 displacement transducers (6 longitudinal, 2 transversal, 2 diagonal) have been applied on each specimen and 8 displacement transducers (2 longitudinal, 2 transversal, 4 diagonal) for diagonal shear ones.

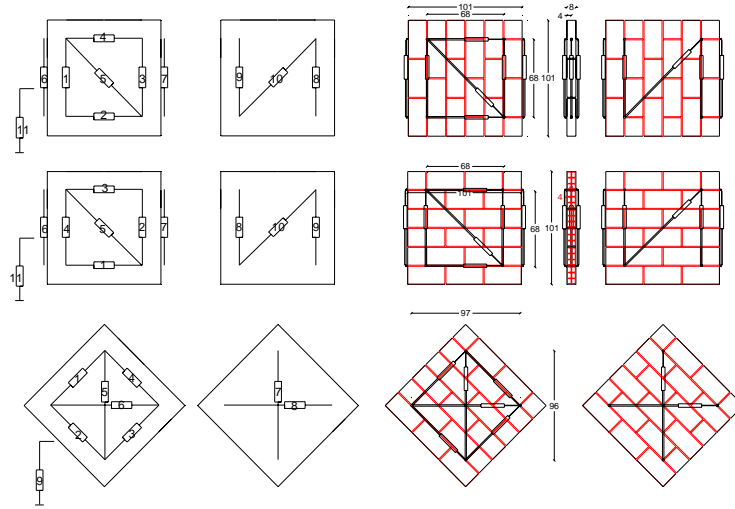


Figure 3. Specimen geometry and displacement transducers disposal for hollow panels: strong direction (top), weak direction (middle) and diagonal direction (bottom)

### 3.1. Test result discussion

Considering specimen geometry and displacement transducers disposal (Figure 2 and Figure 3), the following quantities are determined at each loading step  $n$  in compressive tests:

$$f_{wn} = \frac{F_{wn}}{A_w} \quad \varepsilon_{wln} = \frac{1}{n_l} \sum_{n_l} \frac{\Delta L_{ln}}{L_l} \quad \varepsilon_{wtn} = \frac{1}{n_t} \sum_{n_t} \frac{\Delta L_{tn}}{L_t} \quad \varepsilon_{wdn} = \frac{1}{n_d} \sum_{n_d} \frac{\Delta L_{dn}}{L_d} \quad (3.1)$$

where  $F_{wn}$  current compressive load,  $A_w$  panel gross area perpendicular to compressive load,  $\Delta L$ ,  $L$  and  $n$  are transducer displacement, length and number respectively in longitudinal ( $l \equiv j$ ), transversal ( $t \equiv i$ ) and diagonal [ $d \equiv h(\theta = \pi/4)$ ] directions according to subscript  $l$ ,  $t$  and  $d$ . If peak (maximum) strength is determined,  $f_{wm}$ , elastic characteristics can be defined as secant characteristics in the elastic range:

$$\Delta f_{wl} = (\alpha_2 - \alpha_1) f_{wm} \quad \Delta \varepsilon_{wl} = \varepsilon_{wl} f(\alpha_2 f_{wm}) - \varepsilon_{wl} f(\alpha_1 f_{wm}) \quad (3.2)$$

$$E_{wl} = \frac{\Delta f_{wl}}{\Delta \varepsilon_{wl}} \quad \nu_{wtl} = -\frac{\Delta \varepsilon_{wt}}{\Delta \varepsilon_{wl}} \quad (3.3)$$

where  $j$ -direction is (vertical) load direction and  $i$ -direction the normal (horizontal) direction, as above said. In this paper the elastic loading branch between 25% ( $\alpha_1 = 0.25$ ) and 50% ( $\alpha_2 = 0.50$ ) of the failure load is considered both for compressive and shear tests. Diagonal strains ( $\theta = \pi/4$ ) can be used in order to control the step by step strain compliance: using Eqn. (2.4) the longitudinal strain error  $\hat{\varepsilon}_{wn}$  can be determined as:

$$\hat{\varepsilon}_{wn} = \varepsilon_{wdn} - (\varepsilon_{wtn} \cos^2 \theta + \varepsilon_{wln} \sin^2 \theta) = \varepsilon_{wdn} - \frac{\varepsilon_{wtn} + \varepsilon_{wln}}{2} \quad (3.4)$$

In the case of shear test, at each loading step  $n$  shear stress  $\tau_{wn}$  and shear strain  $\gamma_{wtn} = 2\varepsilon_{wtn}$  can be obtained by means of longitudinal, transversal and diagonal transducer measures:

$$\tau_{wn} = \frac{\sqrt{2} F_{wn}}{2 A_w} \quad \gamma_{wtn} = \frac{1}{n_t} \sum_{n_t} \frac{\Delta L_{tn}}{L_t} - \frac{1}{n_l} \sum_{n_l} \frac{\Delta L_{ln}}{L_l} = \varepsilon_{wt} - \varepsilon_{wl} \quad G_{wtn} = \frac{\Delta \tau_{wtn}}{\Delta \gamma_{wtn}} \quad (3.5)$$

Transversal displacement transducers can be used in shear tests in order to control Poisson's ratio value in this direction: while longitudinal strain path is constant, the transversal one can be assumed as maximum at specimen center,  $\varepsilon_{wt \max}$ , and zero at specimen edges. If  $\varepsilon_{wt}$  of Eqn. (3.5) is assumed linearly variable, maximum transversal strain can be calculated and an equivalent Poisson's ratio  $\nu_{wd}$  determined:

$$\varepsilon_{wt \max} = \left(1 - \frac{\sqrt{2} L_t}{4 L_w}\right)^{-1} \varepsilon_{wt} \quad \nu_{wd} = -\frac{\Delta \varepsilon_{wt \max}}{\Delta \varepsilon_{wl}} \quad (3.6)$$

Also in this case diagonal strains ( $\varepsilon_{whn} = \varepsilon_{wdn}(\theta = \pi/4)$ ,  $\varepsilon_{wkn} = \varepsilon_{wdn}(\theta = 3\pi/4)$ ) can be used in order to control the step by step strain compliance by means of the diagonal strain error:

$$\widehat{\varepsilon}_{wdn} = \varepsilon_{whn} - \varepsilon_{wkn} \quad (3.7)$$

In Table 2 elastic characteristics of panels, i.e. terms of elastic stiffness matrix, are summarized; for a better understanding subscript *s* stands for strong (hollow) direction, while *w* for weak (normal) direction. In Table 2 the equivalent Poisson's ratio  $\nu_{wd}$  is also shown. Notice that experimental elastic moduli are at least double than Code provision, Eqn. (2.11), a greater difference can be detected in the shear modulus of hollow panels (almost eighty percent of the elastic modulus). Thereafter for semi-solid panels and for hollow panels the average Poisson's ratios is much more greater than both the Code value ( $\nu_w = 0.25$ ) and the maximum elastic value ( $\nu_{\max} = 0.50$ ) of the elastic theory and it is due to non linear behavior of masonry also for low strength level. In spite of this result the compliance matrix **D** is almost symmetrical: Eqn. (2.3) lets to  $D_{ws}/D_{sw} = 0.988$  and  $D_{ws}/D_{sw} = 1.024$  respectively for semi-solid and hollow panels.

In Figure 4 the equivalent diagonal elastic modulus for hollow (left) and semi-solid (right) panels are determined and shown. Using Eqn. (2.6)  $E_{w\theta}(\pi/4) = E_{wd} = 8355$  MPa and  $E_{w\theta}(\pi/4) = E_{wd} = 7693$  MPa are obtained for semi-solid and hollow panels in the diagonal direction respectively. If compliance matrix symmetry is taken into account, diagonal Poisson's ratios are equal to  $\nu_{wd} = 0.625$  and  $\nu_{wd} = 0.565$  for semi-solid and hollow panels. These values are quite similar to those in Table 2 determined using Eqn. (3.6).

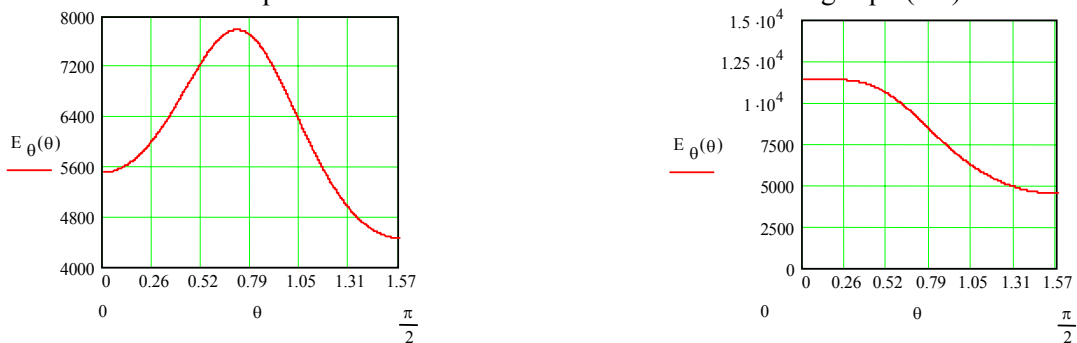


Figure 4. Equivalent diagonal elastic modulus for hollow (left) and semi-solid (right) panels

Finally in Table 2 the proposed homogenization criterion (2.11)-(2.15) is applied with two hypotheses: the 1<sup>st</sup> integrally considering strong and weak elastic modulus obtained as in Eqn. (2.11), the 2<sup>nd</sup> considering elastic modulus experimental values and then deriving shear modulus and Poisson's ratio with (2.12)-(2.14) Eqns.

Table 2. Elastic characteristics of panels

|  | semi-solid panels |                   |                    |                    |                     |                   | hollow panels     |                   |                    |                    |                     |                   |
|--|-------------------|-------------------|--------------------|--------------------|---------------------|-------------------|-------------------|-------------------|--------------------|--------------------|---------------------|-------------------|
|  | $E_{ws}$<br>[Mpa] | $E_{ww}$<br>[Mpa] | $G_{wsw}$<br>[Mpa] | $\nu_{wws}$<br>[-] | $\nu_{ws w}$<br>[-] | $\nu_{wd}$<br>[-] | $E_{ws}$<br>[Mpa] | $E_{ww}$<br>[Mpa] | $G_{wsw}$<br>[Mpa] | $\nu_{wws}$<br>[-] | $\nu_{ws w}$<br>[-] | $\nu_{wd}$<br>[-] |
| experimental                             | 11384             | 4494              | 3135               | 0.85               | 0.34                | 0.70              | 5504              | 4462              | 3852               | 0.40               | 0.32                | 0.62              |
| 1 <sup>st</sup> iph.: $E_w = 1000f_{wk}$ | 6607              | 2582              | 1838               | 0.36               | 0.14                |                   | 2612              | 1797              | 882                | 0.30               | 0.20                |                   |
| 2 <sup>nd</sup> iph.: $E_w = E_{wexp}$   | 11384             | 4494              | 3175               | 0.36               | 0.14                |                   | 5504              | 4462              | 1993               | 0.28               | 0.22                |                   |

In Figure 5 a comparison of diagonal elastic modulus ratios ( $\lambda_1 = E_{w\theta 1hyp}/E_{w\theta}$  solid line,  $\lambda_2 = E_{w\theta 2hyp}/E_{w\theta}$  dot line) is shown. It is possible to note a quite acceptable accuracy for the proposed homogenization criterion if

actual compressive elastic moduli are selected.

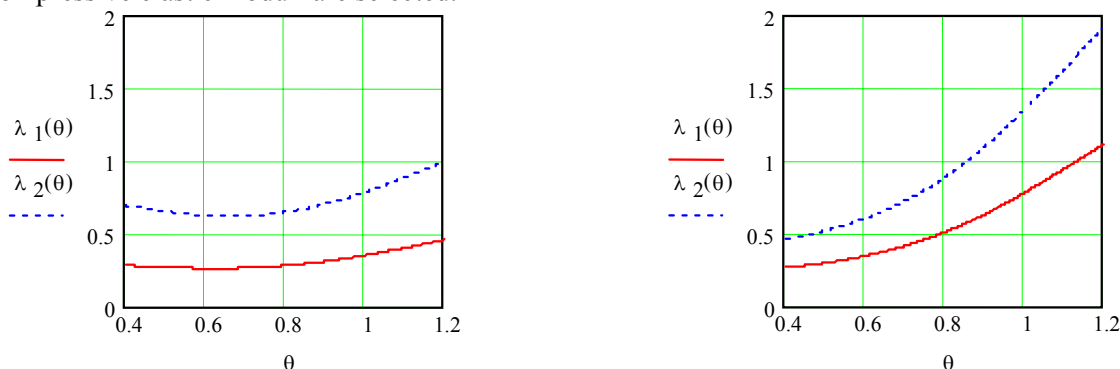


Figure 5. Equivalent diagonal elastic modulus ratios for hollow (left) and semi-solid (right) panels

#### 4. CONCLUSIONS

Many factors make very difficult to define an efficient approach to r.c. infilled frame analysis: in particular it is important to define correctly both structural schemes and constitutive behavior.

So, if a strut model is considered for strong nonlinear analysis, strut geometry and disposal play a relevant role for stress distribution in r.c. frame and, consequently, plastic hinges spreading. In this case constitutive behavior could have a less relevant role (Albanesi et al. 2006).

On the other hand, if an uncracked or quite elastic structural analysis has to be done, an appropriate constitutive behavior has to be used: in this case both brick anisotropy and panel slenderness have to be taken into account. Some criteria are been discussed in this paper.

Particularly, a homogenization criterion to evaluate equivalent diagonal elastic modulus for hollow and semi-solid panels, proposed in the past, is discussed.

On the basis of this criterion two hypotheses have been carried out to determine infill masonry behavior: the first using a conventional method for elastic modulus evaluating, the second using actual elastic modulus results of a wide test campaign.

It is shown that the proposal to use the actual compressive elastic modulus carried to results quite similar to experimental data; these results will be used by authors for infill equivalent strut calibration in analyses that will be compared with tests on infill frame carried out for the same project These studies are incoming.

#### REFERENCES

- Albanesi, T., Biondi, S., Candigliota, E., Nuti, C. (2006). Local effects modeling of an infilled frame: a three-strut model refinement, *Proc. 2<sup>nd</sup> International fib Congress*, June 5-8, Naples, Paper Id. 3-40.
- Albanesi, T., Bergami, A.V., Nuti, C. (2008.a). Indagine sperimentale e numerica sul comportamento ciclico di telai in c.a. tamponati, *Atti convegno Valutazione e riduzione della vulnerabilità sismica di edifici esistenti in c.a.*, Rome, Italy, May 29-30, 2008. (in Italian)
- Albanesi, T., Bergami, A.V., Biondi, S., Candigliota, E., Nuti C. (2008b). Tests on infilling panels for reinforced concrete frames. *Proc. 6<sup>th</sup> International Conference AMCM'2008 Analytical Models and New Concepts in Concrete and Masonry Structures*, Łódź, Poland, June 9-11, 2008, Paper No. P079
- Anthoine, A. (1995). Derivation of the in-plane elastic characteristics of masonry through homogenization theory. *International Journal Solid Structures*, **32:2**, 137-163.
- Bazant, Z. P. (1983). Comment on orthotropic models for concrete and geomaterials. *Journal of Engineering Mechanics*, **109:3**, 849-865.
- Biondi, S., Candigliota, E., Nuti, C. (2002). Tests on different infilled specimens: a critical review of Code ultimate state criteria, *Proc. 12<sup>th</sup> European Conference on Earthquake Engineering*, London, U.K., September 9-13, 2002, paper 748.
- Gambarotta, L., Lagormarsino, S. (1997). Damage models for the seismic response of brick masonry shear walls. Part I: The mortar joint model and its applications - Part II. The continuum model and its applications. *Earthquake Engineering and Structural Dynamics*, **26:3**, 423-462.
- Pietruszczak, S., Niu, X. (1992). A mathematical description of macroscopic behaviour of brick masonry. *International Journal Solid Structures*, **29:5**, 531-546
- Tassios, T. P. (1988). *Meccanica delle murature*, Liguori Editore, Napoli, Italy, (in Italian).